Journal of Thermal Analysis and Calorimetry (2023) 148:3117–3127
https://doi.org/10.1007/s10973-022-11545-8

Optimization of a boron nitride nanotubes nanofluid-cooled microchannel heat sink at different concentrations

Nur Liyana Nabihah Yusof[1] · Hielfarith Suffri Shamsuddin[1] · Patrice Estellé[2] · Normah Mohd-Ghazali[1]

Received: 2 January 2022 / Accepted: 25 July 2022 / Published online: 9 September 2022

Abstract

The microchannel heat sink (MCHS) has become the most relevant micro-heat exchanger for a small area in need of an effective high heat removal system. However, heat dissipation from the microchips where the MCHS is utilized—the microprocessor and microcontroller—is getting higher with the sizes getting smaller. A more effective coolant is needed to address the increasing heat load from the microchip and nanofluid, nanosized particles dispersed in a base fluid, is among those explored. This paper reports a new potential use of non-metallic nanofluid, boron nitride nanotube (BNN), that is capable of improving the overall performance of a rectangular MCHS. A heuristic method, multi-objective genetic algorithm (MOGA), is employed to simultaneously minimize the thermal resistance and pressured drop of a boron nitride nanotubes (BNN) nanofluid-cooled MCHS to obtain optimized dimensions at various mass concentrations. The method is capable in achieving conflicting objectives, minimization of the thermal resistance and the pressure drop; an increase in the former decreases the latter and vice versa. In addition, experimental thermophysical properties of the BNN nanofluid are used to provide reliability to the optimization outcomes in identifying the best BNN concentration for cooling of a MCHS at 50 °C. The optimization results showed that as the thermal resistance decreases, the pressure drop decreases. For mass concentrations of 0.001, 0.003, 0.005, 0.01 and 0.03% the thermal resistance is the lowest, 0.0711 K/W at 0.01 mass.%. at 0.0115 W. The thermal resistance is lowered by 5.34% compared to water for the same operating conditions. These results indicate the great potential of BNN nanofluid as a coolant in the electronics cooling system. Optimization with the MOGA provides a fast analysis into the potentials of any coolants for MCHS applications as shown here, reliability being provided by experimentally obtained thermophysical properties.

Keywords Microchannel heat sink · Multi-objective genetic algorithm · Optimization · Boron nitride nanotubes nanofluid

List of symbols

C_p	Specific heat (J k g^{-1} K^{-1})
D_h	Hydraulic diameter (m)
H	Heat sink height (m)
H_{av}	Heat transfer coefficient (W m^{-2} K^{-1})
t	Substrate thickness (m)
H_c	Channel height (m)
w_c	Channel width (m)
ww	Wall width (m)
L	Heat sink length (m)
W	Heat sink width (m)
R_{total}	Total thermal resistance (K W^{-1})
k_s	Thermal conductivity (W m^{-1} K^{-1})
Nu	Nusselt number
Re	Reynolds number
k_{hs}	Thermal conductivity(W m^{-1} K^{-1})
V_{mnf}	Velocity inside the microchannel (ms^{-1})
f	Friction factor
Pp	Pumping power (W)
ΔP	Pressure drop (Kpa)

Greek symbols

α	Hydraulic diameter
β	Wall width to channel width ratio
ρ_f	Density of nanofluid (k g m^{-1})
μ_f	Viscosity of nanofluid (k g s^{-1} m^{-1})
η	Fin efficiency

✉ Nur Liyana Nabihah Yusof

✉ Patrice Estellé

✉ Normah Mohd-Ghazali
normah@mail.fkm.utm.my

[1] School of Mechanical Engineering, Faculty of Engineering, Universiti Teknologi Malaysia, UTM Johor Bahru, 81310 Johor, Malaysia

[2] LGCGM, University of Rennes, 35000 Rennes, France

Subscripts

h_s	Heat sink
c	Channel
nf	Nanofluid
w	Wall
f	Fluid of coolant
s	Substrate

Introduction

Microchannel heat sink is an established heat removal system that is capable of removing high heat loads dissipated from the electronic chips. With emerging advanced technology, the system needs to remove a highly concentrated heat source with the miniaturization of today's electronic chips and their increasing power density. Designing a good thermal management system has been a series of challenges to researchers and engineers. Since the significant discovery made by Tuckerman and Pease [1], numerous studies had been done to improve the performance of the microchannel heat sink (MCHS). The improvement had been made with different coolants and geometries of the heat sink. Innovation in geometry is limited to the manufacturers' capability and associated cost. On the other hand, many studies had been completed theoretically, experimentally and numerically on the MCHS using different coolants to further improve its heat removal capability. The MCHS cooling system generally comprises of parallel microchannels positioned atop the chip, with an adiabatic plate covering them to preserve the coolant. The MCHS designed by Tuckerman and Pease [1] proved that a MCHS was capable of removing 790 W/cm^2 of heat. However, conventional cooling with gas, air, and water for a MCHS may no longer be able to address increasing heating issues as high as 1000 W/cm^2 [2]. Thus, this has encouraged researchers to explore new coolants to remove heat effectively and efficiently, one of them being nanofluids. Nanofluid is a liquid consisting of solid nanoparticles combined with a common base—water, ethylene glycol, and oil. The presence of the suspended nano-sized particles of high thermal conductivity improves the heat removal capability of the base fluid.

One of the earliest modeling of a nanofluid-cooled MCHS was in 2007 [3]. The analytical study with the porous medium model with copper–water (Cu-H_2O) and carbon nanotube-water (CNT-H_2O) nanofluids showed compelling results in heat transfer performance and pressure drop when compared to water as both nanofluid-cooled MCHS improved significantly. An experimental study that same year showed that for volume fractions 0.2 to 0.4% of CuO-H_2O nanofluid, the MCHS performed better than the water-cooled unit agreeing well with the theoretical predictions, although agglomerations and depositions occurred with time [4]. Another study proved that nanoparticles Al_2O_3 suspended in water enhanced the convective heat transfer coefficient in the thermally fully developed regime, at the low volume fraction between 0.01 and 0.3 vol% [5]. The heat transfer coefficient of the water-based Al_2O_3 nanofluids was increased by 8 at 0.3 vol% under a fixed Reynolds number (Re = 1000) compared with that of pure water. Nanofluids with metallic or its oxides nanoparticles commonly investigated are copper [3, 4, 6], titanium [7–10], silver [8, 11], and aluminum [2, 5, 7, 12–14]. A review of the flow and heat transfer behavior of nanofluids in microchannel heat sinks has been done by Kumar et al. [15]. It was concluded that nanofluids presented a promising potential as an effective coolant in removing heat with Cu-H_2O being more attractive than Al- H_2O nanofluid. The enhancement in heat transfer mainly depends on the type of nanoparticle, their volume fraction, shape and size, and the aspect ratio of the nanotube itself.

The last decade has seen the analysis of the thermal performance of the MCHS being completed using computational fluid dynamics (CFD) and optimization with a heuristic approach. The former may provide detailed thermo-fluid profiles while the latter can generate optimal sets of solutions for multiple conflicting objectives. Each has its own advantages. The CFD approach allows a look at the fluid and thermal vectors associated with the coolant investigated in any particular complex geometry explored. The CFD study with laminar nanofluid SiO_2, Al_2O_3, ZnO, and CuO dispersed in pure water in a microchannel heat sink (MCHS) with V-Type inlet/outlet arrangement is one such example [16]. Volume fractions of 1, 1.5, and 2% and three distinctive nanoparticle diameters of 30, 40, and 60 nm were employed. The results indicated that the SiO_2 nanofluid had the uppermost heat transfer rate compared to other tested nanofluids. Meanwhile, the optimization with a heuristic procedure opens up possibilities for simultaneous minimization of the conflicting desired outcomes of thermal and hydrodynamic performances; the increased in one decreases the other. The optimization of two nanofluids with different volume fractions of 1, 3, 5, 7, and 9% of SiC-H_2O and TiO_2- H_2O in a MCHS had been studied by Adham et al.[8] using multi-objective genetic algorithm. It was found that both nanofluids had a greater performance in terms of thermal resistance in comparison with pure water under the same operating conditions. The nanoparticles volume fraction affected the thermal resistance and pumping power, the decrease in the MCHS thermal resistance decreased the pumping power; optimized dimensions of the channels were obtained.

Initially, metallic nanoparticles were the best alternative since they increase the coolant thermal conductivity tremendously. However, continued studies had suggested that a high concentration of metallic nanoparticles causes a high friction factor in the flow which resulted in a higher

pressure drop leading to a higher pumping power. Consequently, utilization of non-metallic nanofluids has been investigated apart from water and gaseous coolants [17]. The convective heat transfer and fluid dynamics performance of silicon dioxide, SiO_2, nanoparticles in combination with ethylene glycol and water as the base fluid at a fixed Reynolds number (Re = 10, 000) was found to increase the heat transfer coefficient. Pressure loss was observed to still increase as the concentration of nanofluid increased [18]. Halelfadl et al. [19] utilized carbon nanotube (CNT) based nanofluid in their optimization analysis of the rectangular MCHS, comparing the outcomes with those from Tuckerman and Pease [1]. Their results showed improved thermal and hydrodynamic performance of the CNT nanofluid-cooled MCHS. Other types of non-metallic coolants have also been investigated up to recently reporting improved heat transfer capability of the MCHS [20–22].

A recent study had looked at the effect of surfactant, an additive needed to stabilize the nanoparticles in a nanofluid, on the thermal performance and pressure drop in a MCHS [23]. At 30 °C, a significant increase in the thermal performance of the boron nitride nanotubes (BNN) nanofluid-cooled MCHS studied was observed after the addition of the surfactant Triton X-100, with no change after adding the nanoparticles. At 50 °C, however, it was shown that the lowering of the thermal resistance was attributed to the BNN nanoparticles. However, the effects of a particular surfactant added to nanofluid have been rarely investigated. Without the additive, the nanoparticles will agglomerate which reduces the surface area, later being deposited onto the channel floor [4]. Experimental studies completed on the thermophysical properties on CNT nanofluids have concluded that a surfactant is necessary for nanofluid stability for a long period of time else clogged channels occur due to the agglomeration of the nanoparticles [24]. The properties may deviate under certain conditions. Consequently, experimentally obtained thermophysical properties should be used for performance analysis to provide a higher reliability to the outcomes.

This paper reports the results of an optimization approach on the dimensions of a MCHS using a heuristic method; simultaneous minimization of its thermal resistance and pumping power, two conflicting objectives–decreasing of one result in an increase in the other and vice versa. Multi-objective genetic algorithm (MOGA) was used to investigate the thermal and hydrodynamic performance of a BNN nanofluid-cooled MCHS at various concentrations of the BNN at 50 °C. MOGA has been frequently used in the performance modeling of a MCHS [25–28]. Furthermore, thermophysical properties issued from experiments have been used for providing reliability to the optimization modeling outcomes which can lead to the best concentration identification for the MCHS [29].

Theory

A schematic structure of the rectangular MCHS analyzed is shown in Fig. 1. The unit has dimensions of $L = 1$ cm, $W = 1$ cm, $H_c = 320$ µm, $t = 213$ µm, and H of 533 µm [1]. The model applied here follows that used by many previous researchers [1, 3, 8, 13, 17, 19, 22, 23, 25]. A constant heat flux is assumed on the bottom of the MCHS while the top is covered with an adiabatic plate. There is no heat lost from the sides of the MCHS unit. Coolant at the flow rate of $G = 4.7 \times 10^{-6}$ m^3/s flows through the MCHS unit and fully developed laminar flow is assumed, the channels being short. Optimization of the thermal performance and hydrodynamic performance of the rectangular MCHS using boron nitride nanotubes (BNN) nanofluid was completed to determine the design parameters that produce minimum thermal resistance to heat transfer as well as minimum pressure drop. The latter has been established to increase when the former decreases and vice versa.

A uniform heat flux is presumed to be transferred from the bottom of the MCHS described in Fig. 1 that is directly in contact with the heat source, the electronic chip. A working fluid flows through the series of parallel channels along the length of the MCHS to remove the heat flux generated. The thermal performance of the MCHS is measured by its thermal resistance. Previous studies stated that as the thermal resistance decreases, the pressure drop would increase and vice versa. To achieve a high overall performance, both performance parameters must be as low as possible. Thus, optimization of the thermal performance and hydrodynamic performance of a rectangular MCHS cooled with boron nitride nanotubes (BNN) nanofluid is investigated to determine the optimum results. Since the channel walls are generally very thin, they are treated as fins. These assumptions are considered to assist in the analysis:

- The flow is laminar and steady state.
- The thermophysical properties are constant at 50 °C.
- The flow is fully developed and incompressible.
- The analysis is one-dimensional.
- The temperature is uniform over the cross section.
- The interior walls of the microchannel are assumed to be smooth.
- The averaged heat transfer, *h,* is used for the cross section.
- The radiation heat transfer is negligible.
- The gravitational force is negligible.

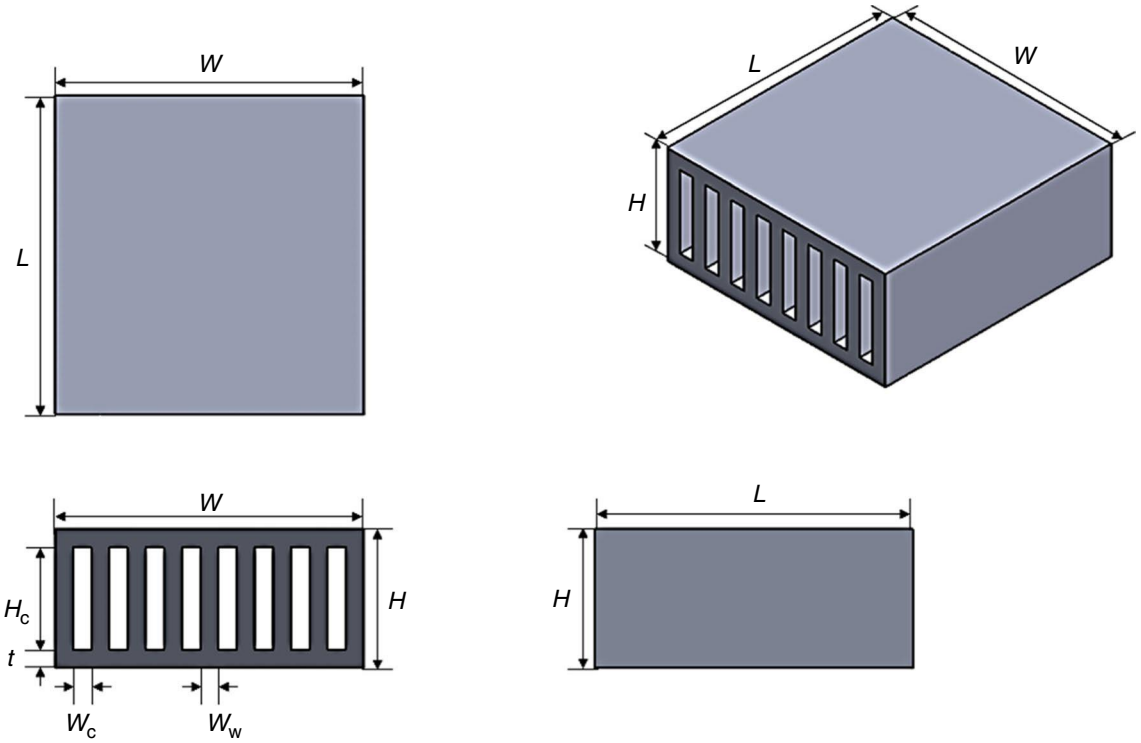

Fig. 1 Rectangular MCHS

Thermal resistance model

The total thermal resistance is comprised of the resistance posed by the substrate below the channels, R_{cond}, resistance to the convective heat transfer, R_{conv}, and resistance due to the coolant heat capacity, $R_{cap,}$ where the resistances are assumed to be in series [30].

The overall thermal resistance is generally expressed as

$$R_{total} = \frac{\Delta T}{q'' A_s} \tag{1}$$

where ΔT is the temperature difference between the peak temperature in the heat sink at the outlet, $T_{o,max}$, and the fluid inlet temperature,T_{in}. q'' is the constant uniform heat flux and A_s is the area of heat sink. With a constant heat flux and surface area of the heat sink, a small R_{total} would mean a small temperature difference, which indicates a good heat removal capability. The total thermal resistance according to the thermal resistance model [22] equivalent to (1) can be determined from

$$R_{total} = R_{cond} + R_{conv} + R_{cap} \tag{2}$$

The conductive thermal resistance is a function of the thickness of the substrate, as the heat flux is applied through the base of the MCHS; it can be expressed as

$$R_{cond} = \frac{t}{k_{hs}(LW)} \tag{3}$$

with t being the substrate thickness, k_{hs} the thermal conductivity of the heat sink, L the length and W the width of the MCHS unit. The generated heat by the electronic chip will be first conducted through the base of the MCHS. Next, heat is resisted by the convective thermal resistance from the base to the coolant

$$R_{conv} = \frac{1}{h_{av} A_{eff}} \tag{4}$$

where h_{av} is the heat transfer coefficient and A_{eff} is the total effective area for the convective heat transfer defined as

$$A_{eff} = nL\left(w_c + 2\eta H_c\right) \tag{5}$$

w_c is the width of channel while H_c is the height of the channel. The term n is the number of microchannels defined as

$$n = \frac{W}{w_w + w_c} \tag{6}$$

The term w_w is the width of the channel wall and η is the fin efficiency where the wall can be treated as a fin by assuming it as an adiabatic fin tip with the fin efficiency defined as

$$\eta = \frac{\tanh\left(mH_c\right)}{mH_c} \tag{7}$$

$$m = \sqrt{\frac{2h_{av}}{k_s w_w}} \tag{8}$$

The capacitive thermal resistance existed within the coolant as it absorbs and removes the heat in the channels

$$R_{cap} = \frac{L}{Cp_{nf} G \rho_{nf}} \tag{9}$$

where ρ_{nf} is the density of the nanofluid in this study and Cp_{nf} is the capacitance of the nanofluid. The term G is the volumetric flow rate and is defined as

$$G = nH_c w_c V \tag{10}$$

where V is the average velocity of coolant inside the MCHS. In this investigation, the channel width-to-channel height ratio, α, and channel wall width-to-channel width ratio, β, are regarded as the variables to be optimized

$$\alpha = \frac{H_c}{w_c} \tag{11}$$

$$\beta = \frac{w_w}{w_c} \tag{12}$$

The hydraulic diameter and Reynolds number used to determine the flow regime are defined by

$$D_h = \frac{4H_c w_c}{2\left(H_c + w_c\right)} = \frac{2}{1+\alpha} H_c \tag{13}$$

$$Re = \frac{\rho_f V D_h}{\mu_f} = \frac{2\rho_f G}{\mu_f n H_c} \frac{\alpha}{\alpha + 1} \tag{14}$$

$$Nu = 2.253 + 8.164\left(\frac{\alpha}{1+\alpha}\right)^{1.5} \tag{15}$$

$$Nu = \frac{h_{av} D_h}{k_f} \tag{16}$$

By substituting Eqs. (5) through (8) and Eqs. (10) through (16), into Eqs. (3), (4) and (9), the total thermal resistance is obtained [9]. The simplified thermal resistance in terms of the variables α and β are

$$R_{cond} = \frac{t}{k_{hs}} \tag{17}$$

$$R_{conv} = \frac{1}{h_{av}} \frac{1+\beta}{1+2\alpha\eta} \tag{18}$$

$$R_{cap} = \frac{L}{Cp_{nf}\mu_{nf}} \frac{2}{Re} \frac{1+\beta}{1+\alpha} \tag{19}$$

The total thermal resistance to the heat generated through the MCHS is sum of the Eqs. (17), (18), and (19) which can be written as [4–6]:

$$R_{total} = \frac{L}{Cp_{nf}\mu_{nf}} \frac{2}{Re} \frac{1+\beta}{1+\alpha} + \frac{1}{h_{av}} \frac{1+\beta}{1+2\alpha\eta} + \frac{t}{k_{hs}(LW)} \tag{20}$$

For the hydrodynamic performance, it is evaluated using the pressure drop or pumping power [22, 23]. The total pressure drop across the MCHS can be expressed as

$$\Delta P_{tot} = P1 + P2 \tag{21}$$

where P1 and P2 in Eq. (21) are described as

$$P1 = f_{hs} \frac{(1+\alpha)L}{2H_c} \rho_{nf} \frac{V_{mnf}^2}{2} \tag{22}$$

$$P2 = \left[1.79 - 2.23\left(\frac{1}{1+\beta}\right) + 0.53\left(\frac{1}{1+\beta}\right)^2\right] \rho_{nf} \frac{V_{mnf}^2}{2} \tag{23}$$

where the term of f_{hs} is the friction factor of the laminar flow and velocity is represented by

$$f_{hs} = \frac{64}{Re} \tag{24}$$

$$V_{mnf} = \frac{Re\,\mu_{nf}}{\rho_f H_c} \tag{25}$$

In terms of the evaluation for the pumping power required to drive the coolant, the equation involved is given by

$$P_p = \Delta P_{tot} G \tag{26}$$

Equations (20) and (26) are to be minimized. However, as discussed earlier, a decrease in the total thermal resistance comes at the expense of a higher pressure drop, consequently, the pumping power and vice versa. With a heuristic approach, simultaneous minimization is made possible with a combination of optimized parameters and this study utilized MOGA to attain this.

Table 1 Mathematical validation result

Model	Alpha, α	Beta, β	R (K/W)	Δ*P*	R %	Δ*P* %
T&P [1]	5.714	0.7857	0.11	0.486	–	–
Current model	5.714	0.7857	0.1059	0.895	3.73	8.41

Table 2 Algorithm parameter used in the study

Criteria	Description
Size of population	50
Number of variables	2
Number of objectives function	2
Selection function	Arithmetic
Crossover function	Uniform
Stopping criteria	1×10^{-6}

Table 3 Design variables limit

Limits	Alpha, α	Beta, β
Upper	10	0.1
Lower	1	0.01

Methodology

In the current study, the mathematical validation is performed to ensure that the thermal resistant model chosen is reliable. The results were compared with the landmark study of Tuckerman and Pease [1].

Mathematical validation

Table 1 shows the mathematical validation results of the current model against the experimental results from Tuckerman and Pease [1]. The results of the current model showed good agreement with Tuckerman and Pease's model in terms of the thermal resistance and pressure drop. The relative uncertainty of the thermal resistance and pressure drop of the MCHS are then determined. They are found to be 3.73 and 8.41%, respectively. In the current model, the coolant used was saturated water [30] while in the previous study it was deionized water. Both working fluids were operated at 23℃. The difference in the thermophysical properties of the coolant slightly affected the outcome of the thermal resistance and hydrodynamic performance of the MCHS.

Optimization with water using multi-objective genetic algorithm (MOGA)

In the current study, multi-objective genetic algorithm (MOGA) optimization on a MCHS was carried out on the two conflicting objective functions which are the thermal resistance and pumping power, an increase in one will cause a decrease in the other and vice versa. To simultaneously minimize both objectives, MOGA was utilized to search for the best combinations of the design variables, α and β. As the solution of a multi-optimization process is not a single solution, many possible solutions are generated with a Pareto optimal solution. MOGA is available in MATLAB (R2019b) software toolbox which is utilized in the current study.

Several algorithm parameters and the design variables limits must be provided in order for the algorithm to be applied accurately and efficiently. The criteria involved have been based on a past research [21] and are listed in Tables 2 and in Table 3. Table 4 shows the comparison of the outcomes between the optimized and non-optimized water-cooled MCHS.

Subsequently, optimization was done on a BNN nanofluid-cooled MCHS. Following the advice of Mare et al. [24], experimental thermophysical properties at 50 °C at various volume concentrations were utilized, as listed in Table 5 [29].

Results and discussion

Table 6 compares the thermal resistance and pumping power of the MCHS shown in Fig. 1, cooled with water and that with BNN nanofluids at 0.001, 0.003, 0.005, 0.01, and 0.03% in mass content at 50 °C. For this analysis, a constant value of channel height, H_c and volumetric flow, G, was set at 320 μm and 4.7 × 10–6 m^3s^{-1}, respectively. The values follow that of Tuckerman and Pease [1] experimental study. A search area of 50 has been chosen in this study as when population of 50, 100 and 150 were compared; the minimum and maximum of the thermal resistance and pressure drop were almost the same for all three populations with the upper and lower limits of α and β according to those listed in Table 3. Hence, the optimization procedure was set with a population of 50 as less search operation was required.

The Pareto front of Fig. 2 presents the relationship between the thermal resistance and pumping power for water and BNN nanofluids as a result of the optimization with MOGA. Each point is an optimal solution associated with a set of optimized α and β where limits are according to Table 3. The Pareto front is a result of the simultaneous minimization of the thermal resistance and pumping power of the BNN nanofluid-cooled MCHS. According to

Table 4 Comparison of optimization using water

Description	Alpha, α	Beta, β	R (K/W)	Δ*P*(psi)	R %	Δ*P* %
Non-optimized	5.714	0.7857	0.1059	0.895	–	–
Optimized	5.44107	0.01	0.0919	0.3337	13.2	6.2

Table 5 Thermophysical properties of BNN nanofluid at 50 °C [29]

Fluid	H2O	0.001 mass.%	0.003 mass.%	0.005 mass.%	0.01 mass.%	0.03mass.%
k (W/mK)	0.56	0.567	0.566	0.577	0.595	0.596
ρ (kg/m^3)	989.8	990.2	990.4	990.5	990.7	990.9
C_p(W/kgK)	4.0041	4.115	4.1513	4.1717	4.2885	4.2456
μ (Ns/m^2)	0.5051	0.4942	0.49298	0.48897	0.49107	0.504

Table 6 Optimization results of BNN nanofluids at 50 °C

Limits	α (1–10)	β (0.01–0.1)	Thermal resistance (K/W)	Pumping power (psi)	Δ R/R(%)
Water	1.00	0.01	0.075138	0.011524	–
0.001%	1.00	0.017	0.074981	0.011487	2
0.003%	1.00	0.01	0.073153	0.011727	2.6
0.005%	1.001	0.011	0.072741	0.011205	3.19
0.01%	1.001	0.01	0.071124	0.011228	5.34
0.03%	1.00	0.01	0.071601	0.011501	4.7

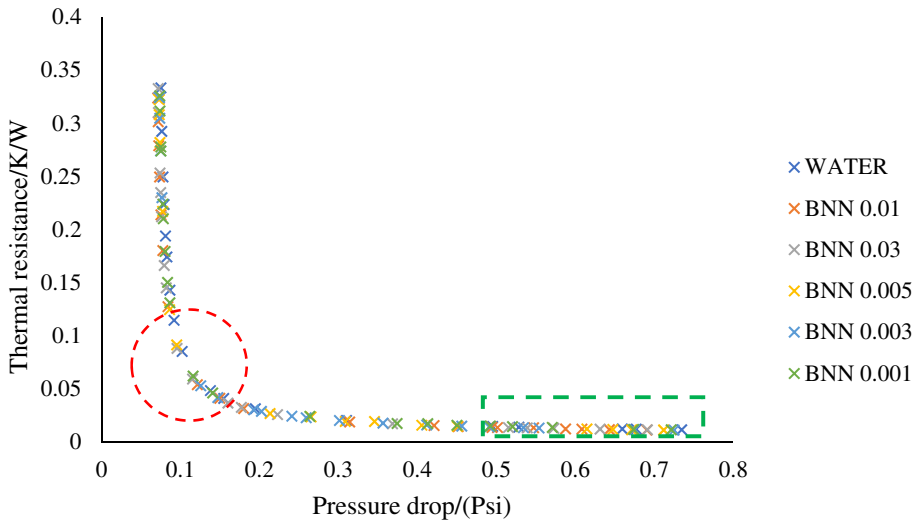

Fig. 2 Optimization of BNN nanofluids at different concentration

the graph, the lowest overall thermal resistance is associated with the highest pumping power for all working fluids investigated. The green rectangle shows the minimize values of thermal resistance at high pressure drop hence the region of the best thermal performance. Meanwhile, the red circle indicates the optimized value that fulfilled both objective functions of low thermal resistance and low pressure drop showing the balance between both parameters. The optimized results reveal that the total thermal resistance at all concentrations of BNN nanofluids is lower than water at 50 °C, as shown in Table 6. The lowest optimized value of thermal resistance for water is 0.075138 °C/W, whereas the lowest optimized value for BNN nanofluid is 0.071124 °C/W at 0.01% of volume concentration. The total thermal resistance reduction between water and BNN nanofluid is 5.34%. The presence of nanoparticles in the BNN nanofluid enhances the cooling capacity of the MCHS. With the increment of heat transfer coefficient, the convective thermal resistance decreases, as has been reported in previous experimental studies [31, 32].

In the current study, the main parameters that affected the geometrical properties are the channel aspect ratio, α, and wall width ratio, β. The channel aspect ratio is the ratio of the heat sink's channel height to channel width, whereas the wall width ratio is the ratio of the heat sink's wall width to channel width. These two parameters are critical in the optimization process for minimizing the total thermal resistance and pumping power. To prevent incoherent results, the channel aspect ratio and wall width ratio are set to a limited range of values according to the limits set in Table 3.

At 50 °C, Fig. 3 portrays the relationship between the total thermal resistance and channel aspect ratio. According to the graph's trend, as the channel aspect ratio increases, the total thermal resistance decreases. Higher channel aspect ratio values resulted in lower total thermal resistance values for BNN nanofluid-cooled MCHS. The thermal resistance of all nanofluids follows nearly the same trendline for all values of the channel aspect ratio.

The graph's trend indicates a significant decrease in the thermal resistance from channel aspect ratio of 1 to 4. Starting with a channel aspect ratio of 4, the decrement of the thermal resistance is gradual until it approaches a value of 10. In the current study, the height of the channel is held constant. When the channel aspect ratio is increased, the channel width decreases. The decrease in convective thermal resistance is influenced by the decrease in the channel width. As a result, decreasing channel width has a significant impact on the total thermal resistance.

At 50 °C, Fig. 4 shows the relationship between pumping power and channel aspect ratio. It can be seen that as the channel aspect ratio continues to increase, so does the pumping power at all 5 concentrations of BNN nanofluids. A high aspect ratio means a narrower channel which of course

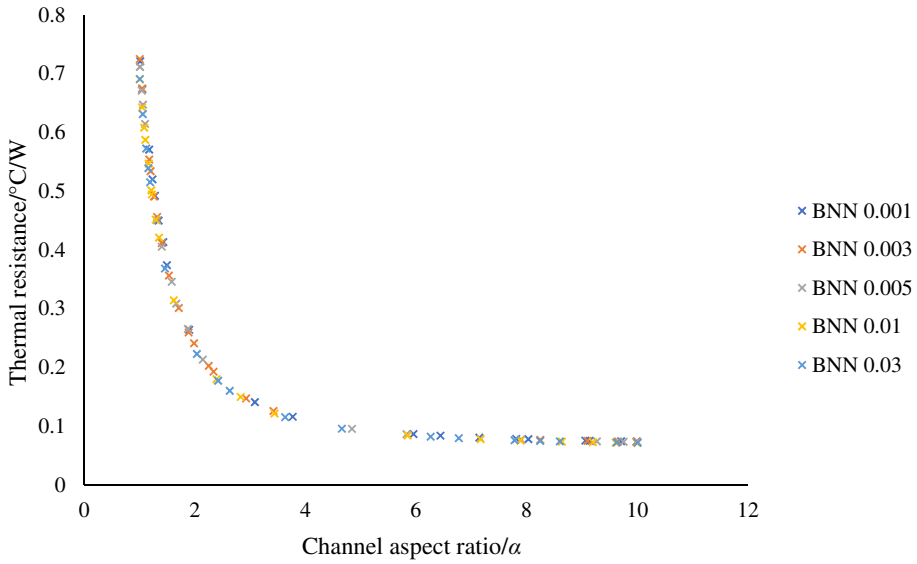

Fig. 3 Thermal resistance vs channel aspect ratio

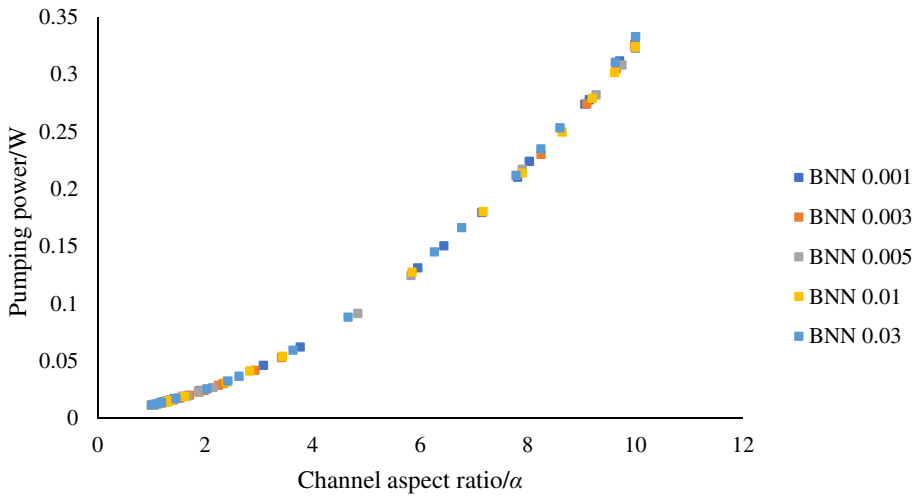

Fig. 4 Pumping power vs channel aspect ratio

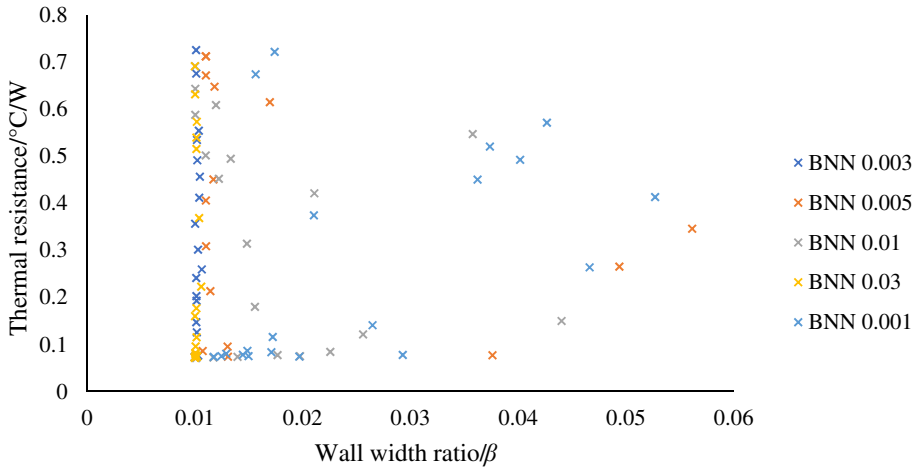

Fig. 5 Thermal resistant vs channel aspect ratio

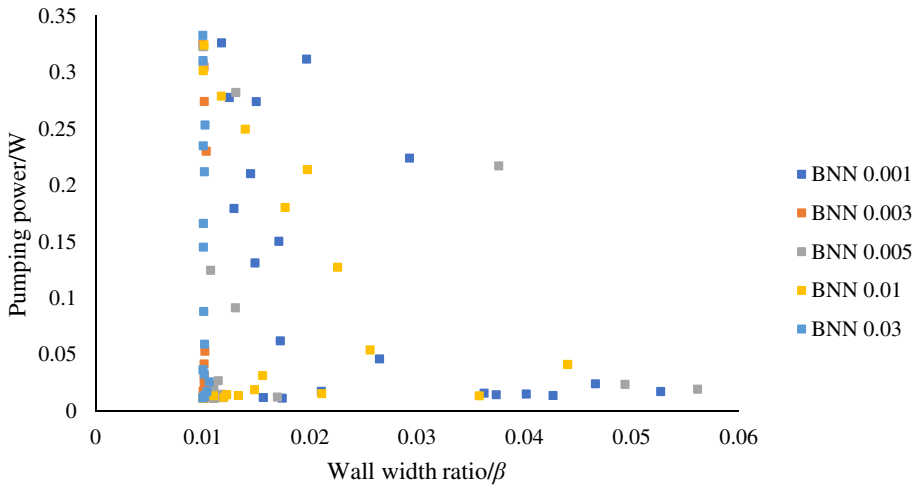

Fig. 6 Pumping power vs wall width ratio

requires a significant increase in pumping power to drive the coolant.

Although the difference in the pumping power between concentrations is not obvious from the graph, Table 6 shows that the BNN nanofluid-cooled MCHS has a higher value of pumping power at 0.03% concentration than at other concentrations at the values of α and β listed. At first, all concentrations exhibit nearly identical behavior patterns; however, at a channel aspect ratio of 6, BNN nanofluids at 0.03% display a slightly higher projection than other concentrations. BNN nanofluids with a concentration of 0.03% have the highest pumping power, followed by BNN with a concentration of 0.001%. This may be because the density and viscosity are highest at 0.03%. As a result, as the channel width narrowed, a high pumping power is required to drive the working fluid.

Figure 5 shows the relationship between the optimized total thermal resistance and wall width ratio, β, of the MCHS at 50℃. It can be observed that most of the points are optimized at the wall width ratio of 0.01. BNN nanofluids at 0.001, 0.003, 0.005, 0.01, and 0.03% showed the same pattern and most of the points are already optimized for $\beta = 0.01$.

Only a few values of the wall width ratio are greater than 0.01 but remain within the range of the upper and lower boundary of β which is at 0.1 and 0.01, respectively. It can be seen that at low values of wall width ratio, the optimum state is achieved. MCHS, it seems, is more sensitive to the channel aspect ratio rather than wall width ratio. The same pattern is observed for the pumping power and wall width ratio, β, relationship, as shown in Fig. 6. It can be observed that most of the points of the wall width ratio are optimized at 0.01 for the five different concentrations.

Conclusions

Simultaneous minimization of the conflicting desired objectives of the thermal resistance and pumping power of a BNN nanofluid-cooled MCHS has been completed. The effects of using 0.001, 0.003, 0.005, 0.01, and 0.03% mass concentration

BNN nanofluid as the coolant in a MCHS under optimal conditions have been obtained with a heuristic approach MOGA utilizing experimentally obtained thermophysical properties for reliability. The optimization procedure took into account design variables of the channel aspect ratio, α, ranging from 1 to 10, while the wall width ratio, β, ranged between 0.01 and 0.1. The study has shown in general the capability of MOGA to explore any new coolants as potentials for MCHS applications and specifically for the BNN nanofluid investigated.

- As the concentration of BNN nanofluid increases, the total thermal resistance of the MCHS decreases, lower by 5.34% at 0.01 concentration, compared to that of water at the same temperature of 50 °C.
- Optimization outcomes showed that as the thermal resistance decreases, the pressure drop increases. The lowest thermal resistance for BNN nanofluid-cooled MCHS investigated is 0.071124 °C/W at the intermediate mass concentration of 0.01%.
- Higher channel aspect ratio values resulted in lower total thermal resistance values for BNN nanofluid-cooled MCHS and consequently a higher pressure drop. The thermal resistance of all concentrations follows nearly the same trendline for all values of channel aspect ratios investigated.

As more coolants are explored in the race for a more efficient and effective MCHS as a heat removal system, a heuristic approach in combination with experimental data of the thermophysical properties can provide reliable design parameters under optimized conditions. Subsequently, experimental studies may complete the analysis into these potential coolants.

Acknowledgements This paper is an extension of our contribution that received the best paper award at the 12th International Meeting on Advances in Thermofluids (IMAT2021). The authors would like to acknowledge the Universiti Teknologi Malaysia (UTM) Research University Grant (UTM) Vot 19H60 in completing this research and the support provided by the Malaysian French Embassy for this collaborative research.

Author's contribution Nur Liyana Nabihah Yusof took part in investigation, visualization, data curation, formal analysis, writing—original draft, review and editing. Hielfarith Suffri Shamsuddin involved in conceptualization. Normah Mohd-Ghazali participated in conceptualization, methodology, supervision, investigation, analysis, writing—original draft, writing—review & editing. Patrice Estellé involved in manuscript review—technical, related experimental study.

References

1. Tuckerman DB, Pease RFW. High-performance heat sinking for VLSI. IEEE Electron Device Lett. 2013;2:126–9. https://doi.org/10.1109/EDL.1981.25367.
2. Mohammed HA, Gunnasegaran P, Shuaib NH. Heat transfer in rectangular microchannels heat sink using nanofluids. Int Commun Heat Mass Transf. 2010;37(10):1496–503. https://doi.org/10.1016/j.icheatmasstransfer.2010.08.020.
3. Tsai TH, Chein R. Performance analysis of nanofluid-cooled microchannel heat sinks. Int J Heat Fluid Flow. 2007;28(5):1013–26. https://doi.org/10.1016/j.ijheatfluidflow.2007.01.007.
4. Chein R, Chuang J. Experimental microchannel heat sink performance studies using nanofluids. Int J Therm Sci. 2007;46(1):57–66. https://doi.org/10.1016/j.ijthermalsci.2006.03.009.
5. Hwang KS, Jang SP, Choi SUS. Flow and convective heat transfer characteristics of water-based Al2O3 nanofluids in fully developed laminar flow regime. Int J Heat Mass Transf. 2009;52(1–2):193–9. https://doi.org/10.1016/j.ijheatmasstransfer.2008.06.032.
6. Azizi Z, Alamdari A, Malayeri MR. Thermal performance and friction factor of a cylindrical microchannel heat sink cooled by Cu-water nanofluid. Appl Therm Eng. 2016;99:970–8. https://doi.org/10.1016/j.applthermaleng.2016.01.140.
7. Mohammed HA, Bhaskaran G, Shuaib NH, Abu-Mulaweh HI. Influence of nanofluids on parallel flow square microchannel heat exchanger performance. Int Commun Heat Mass Transf. 2011;38(1):1–9. https://doi.org/10.1016/j.icheatmasstransfer.2010.09.007.
8. Adham AM, Mohd-Ghazali N, Ahmad R. Optimization of nanofluid-cooled microchannel heat sink. Therm Sci. 2016;20(1):109–18. https://doi.org/10.2298/TSCI130517163A.
9. Xia GD, Liu R, Wang J, Du M. The characteristics of convective heat transfer in microchannel heat sinks using Al2O3 and TiO2 nanofluids. Int Commun Heat Mass Transf. 2016;76:256–64. https://doi.org/10.1016/j.icheatmasstransfer.2016.05.034.
10. Yu J, Kang SW, Jeong RG, Banerjee D. Experimental validation of numerical predictions for forced convective heat transfer of nanofluids in a microchannel. Int J Heat Fluid Flow. 2016;62:203–12. https://doi.org/10.1016/j.ijheatfluidflow.2016.11.001.
11. Sarafraz MM, Nikkhah V, Nakhjavani M, Arya A. Thermal performance of a heat sink microchannel working with biologically produced silver-water nanofluid: Experimental assessment. Exp Therm Fluid Sci. 2018;91:509–19. https://doi.org/10.1016/j.expthermflusci.2017.11.007.
12. Anbumeenakshi C, Thansekhar MR. On the effectiveness of a nanofluid cooled microchannel heat sink under non-uniform heating condition. Appl Therm Eng. 2017;113:1437–43. https://doi.org/10.1016/j.applthermaleng.2016.11.144.
13. Shi X, Li S, Wei Y, Gao J. Numerical investigation of laminar convective heat transfer and pressure drop of water-based Al2O3 nanofluids in a microchannel. Int Commun Heat Mass Transf. 2018;90:111–20. https://doi.org/10.1016/j.icheatmasstransfer.2017.11.007.
14. Wang XD, An B, Lin L, Lee DJ. Inverse geometric optimization for geometry of nanofluid-cooled microchannel heat sink. Appl Therm Eng. 2013;55(1–2):87–94. https://doi.org/10.1016/j.applthermaleng.2013.03.010.
15. Kumar S, Kumar A, Darshan Kothiyal A, Singh Bisht M. A review of flow and heat transfer behaviour of nanofluids in micro channel heat sinks. Therm Sci Eng Prog. 2018;8:477–93. https://doi.org/10.1016/j.tsep.2018.10.004.
16. Abdollahi A, Mohammed HA, Vanaki SM, Osia A, Golbahar Haghighi MR. Fluid flow and heat transfer of nanofluids in microchannel heat sink with V-type inlet/outlet arrangement. Alexandria Eng J. 2017;56(1):161–70. https://doi.org/10.1016/j.aej.2016.09.019.
17. Adham AM, Mohd-Ghazali N, Ahmad R. Cooling of microchannel heat sinks with gaseous coolants. Procedia Eng. 2013;56:337–43. https://doi.org/10.1016/j.proeng.2013.03.128.
18. Kulkarni DP, Namburu PK, Ed Bargar H, Das DK. Convective heat transfer and fluid dynamic characteristics of SiO Ethylene glycol/water nanofluid. Heat Transf Eng. 2008;29(12):1027–1035. https://doi.org/10.1080/01457630802243055.

19. Halelfadl S, Adham AM, Mohd-Ghazali N, Maré T, Estellé P, Ahmad R. Optimization of thermal performances and pressure drop of rectangular microchannel heat sink using aqueous carbon nanotubes based nanofluid. Appl Therm Eng. 2014;62(2):492–9. https://doi.org/10.1016/j.applthermaleng.2013.08.005.
20. Sarafraz MM, Nikkhah V, Nakhjavani M, Arya A. Fouling formation and thermal performance of aqueous carbon nanotube nanofluid in a heat sink with rectangular parallel microchannel. Appl Therm Eng. 2017;123:29–39. https://doi.org/10.1016/j.applthermaleng.2017.05.056.
21. Mohd-Ghazali N, Estellé P, Halelfadl S, Maré T, Siong TC, Abidin U. Thermal and hydrodynamic performance of a microchannel heat sink with carbon nanotube nanofluids: effect of concentration and channel section. J Therm Anal Calorim. 2019;138(2):937–45. https://doi.org/10.1007/s10973-019-08260-2.
22. Shamsuddin HS, Tong LW, Mohd-Ghazali N, Estellé P, Maré T, Mohamad M. Nanofluid-cooled microchannel heat sink with carbon nanotube. Evergreen. 2021;8(1):170–6. https://doi.org/10.5109/4372274.
23. Shamsuddin HS, Estellé P, Navas J, Mohd-Ghazali N, Mohamad M. Effects of surfactant and nanofluid on the performance and optimization of a microchannel heat sink Int. J Heat Mass Transf. 2021;175:121336. https://doi.org/10.1016/j.ijheatmasstransfer.2021.121336.
24. Mare T, Estelle P, Halelfadl S, Mohd Ghazali N. Consideration of carbon nanotube-based nanofluid in thermal transfer. J Teknol. 2016;78(8–4):41–8. https://doi.org/10.11113/jt.v78.9583.
25. Adham AM, Mohd-Ghazali N, Ahmad R. Optimization of an ammonia-cooled rectangular microchannel heat sink using multi-objective non-dominated sorting genetic algorithm (NSGA2). Heat Mass Transf und Stoffuebertragung. 2012;48(10):1723–33. https://doi.org/10.1007/s00231-012-1016-8.
26. Dokken CB, Fronk BM. Optimization of 3D printed liquid cooled heat sink designs using a micro-genetic algorithm with bit array representation. Appl Therm Eng. 2018;143(May):316–25. https://doi.org/10.1016/j.applthermaleng.2018.07.113.
27. Wu R, Zhang X, Fan Y, Hu R, Luo X. A Bi-Layer compact thermal model for uniform chip temperature control with non-uniform heat sources by genetic-algorithm optimized microchannel cooling. Int J Therm Sci. 2019;136:337–46. https://doi.org/10.1016/j.ijthermalsci.2018.10.047.
28. Wang TH, Wu HC, Meng JH, Yan WM. Optimization of a double-layered microchannel heat sink with semi-porous-ribs by multi-objective genetic algorithm. Int J Heat Mass Transf. 2020;149:119217. https://doi.org/10.1016/j.ijheatmasstransfer.2019.119217.
29. Gómez-Villarejo R, Aguilar T, Hamze S, Estellé P, Navas J. Experimental analysis of water-based nanofluids using boron nitride nanotubes with improved thermal properties. J Mol Liq. 2019;277:93–103. https://doi.org/10.1016/j.molliq.2018.12.093.
30. Cengel YA, Gajar AJ. Heat and Mass Transfer, Fundamentals and Applications, 5th Ed. Ch3.2, 59.
31. Ho CJ, Wei LC, Li ZW. An experimental investigation of forced convective cooling performance of a microchannel heat sink with Al2O3/water nanofluid. Appl Therm Eng. 2010;30(2–3):96–103. https://doi.org/10.1016/j.applthermaleng.2009.07.003.
32. Peyghambarzadeh SM, Hashemabadi SH, Chabi AR, Salimi M. Performance of water based CuO and Al2O3 nanofluids in a Cu-Be alloy heat sink with rectangular microchannels. Energy Convers Manag. 2014;86:28–38. https://doi.org/10.1016/j.enconman.2014.05.013.